Spring 2016

Using Raman Spectroscopy To Monitor Photopolymerization

Raymond Ajax Metrulis
Bard College, rm2483@bard.edu

Introduction

The combination of art and science is a deceptively unconventional pair that is the basis of art restoration and conservation. Applying objective scrutiny to subjective material appears to be a volatile process, but both disciplines operate on the same core principles. The scientist relies on the color wheel and complex geometry as does the artist. The quality of light in the environment is crucial for the photographer and the analytical chemist. Art and science encourage careful observation of the environment from all angles and scales to change the world. This method of thinking, the logical left and creative right brain in harmony, is what attracted me to art restoration. I liked the prospect of a career specializing in safeguarding the masterpieces of humanity's past with the scientific progress of the future. As a chemistry major, finding a way to integrate art restoration into my curriculum was troublesome for three years. Over two semesters I had the privilege of extra-curricular research with Professor Sattar by preparing class assignments for Photographic Processes and Paintings and the Composition of Dyes. Studying the chemical make-up of obsolete red dyes and simple light activated printing processes was encouraging, but my proclivity for art restoration was not satiated. While conducting experiments under Professor LaFratta for the 2015 Bard Summer Research Institute (BSRI), I came up with an appropriate topic for my senior thesis that was an extension of my work at the time incorporating Raman spectroscopy and direct laser writing (DLW).

1.1 Photolithography and DLW

The summer research involved elucidating the polymerization mechanism of acrylate monomers patterned with the DLW setup. Photolithography uses light to microfabricate structures with a laser or a photomask by transferring the desired shape on a substrate uniformly covered in a photo-sensitive chemical resist. There are a multitude of photolithography methods to design microstructures, but DLW excels at quick and inexpensive prototyping. Negative photoresist resins solidify when excited with a focused UV beam from a DLW setup to fabricate microstructure prototypes. Resins (a.k.a. photoresists) are spread on a slide mounted on a motorized stage that can be precisely maneuvered via joystick or computer program during exposure from a 405 nm laser focused into a microscope. In order to extract the maximum illumination power, the UV laser is passed through a dielectric beam splitter to polarize the plane of the electric vector parallel to the y-axis. A shutter can be operated either manually or with the same computer program to block the laser. A camera monitors the fabrication in progress with a sub-micron resolution (Figure 1.1).

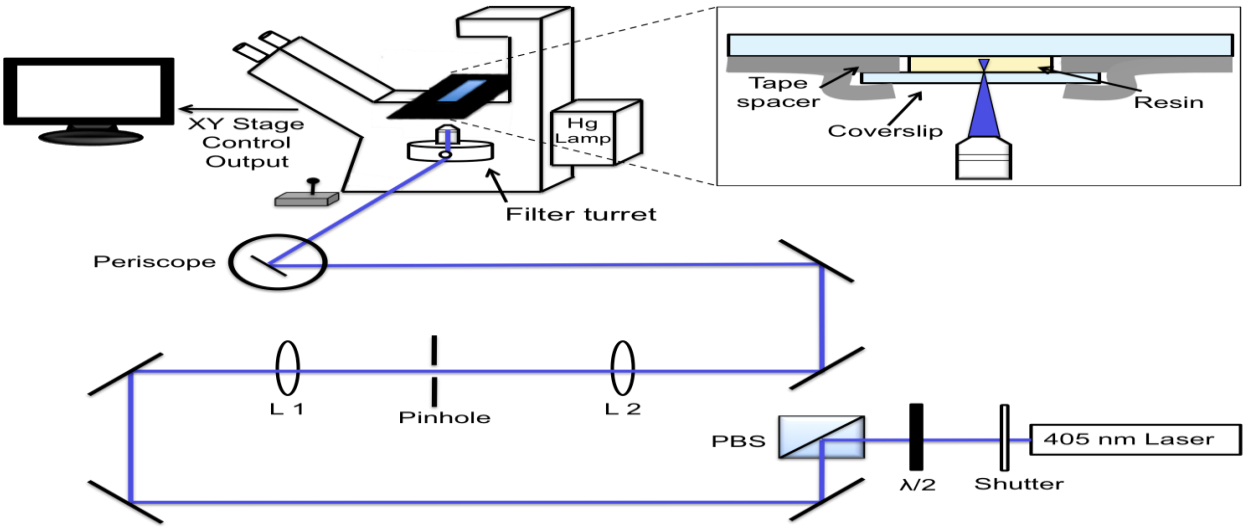

Figure 1.1 Schematic of DLW set-up at Bard College

DLW synthesized microfluidics and lab-on-a-chip devices have many applications in any field of scientific research: aspheric micro-lenses, micro-oscillators, micro-turbines, bioassays, and inkjet printheads to name a few.[1]

1.2 Chemical reaction of acrylate photopolymerization

Liquid photopolymers contain a mixture of monomer, oligomer, and photoinitiator. Light of low wavelength induces polymerization, but highly energetic UV light expedites the process. Some photopolymers already possess chromophores that activate the reaction, while others need the photoinitiator added to induce a chemical change. The chromophore or photoinitiator becomes a highly reactive species, such as a free radical, when exposed to light. The reactive species activates the C=C of the monomer causing the multifunctional monomers to cross-link (Figure 1.2).

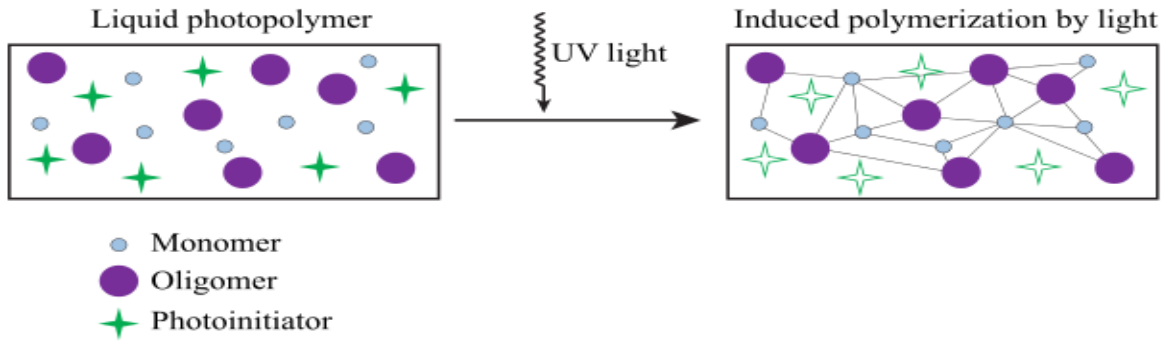

Figure 1.2 Basic photopolymerization mechanism[2]

Photopolymers may require an inhibitor to bind with extra reactive species to prevent undesired reactions from occurring outside of the intended lithographed design. The properties of a photopolymer can be tweaked by balancing the concentrations of oligomer, monomer, photoinitiator, and inhibitor.

1.3 DLW issues: memory effect / proximity effect

There are downsides to DLW that must be understood to improve the utility of the technique. At the micro- and nano- scales, attention to structural detail is crucial. Slight compromises to the integrity of a structure could render it useless and DLW parameters that determine the outcome of structural designs must be expertly tuned. Many variables influence the final product, such as: laser intensity, microscope focus, quality of glass slide, distribution of resin, concentration ratio of photoinitiator to free radical inhibitor to monomer, hiatus time between excitations, and rate of stage movement. Each acrylate monomer behaves and responds differently to these parameters to further complicate operating a DLW setup. One important obstacle of DLW lithography is the memory effect, attributed to catalytic free radicals released during polymerization that diffuse throughout the resin and cause structures to unintentionally compound in size relative to nearby structures polymerized seconds before (Figure 1.3).

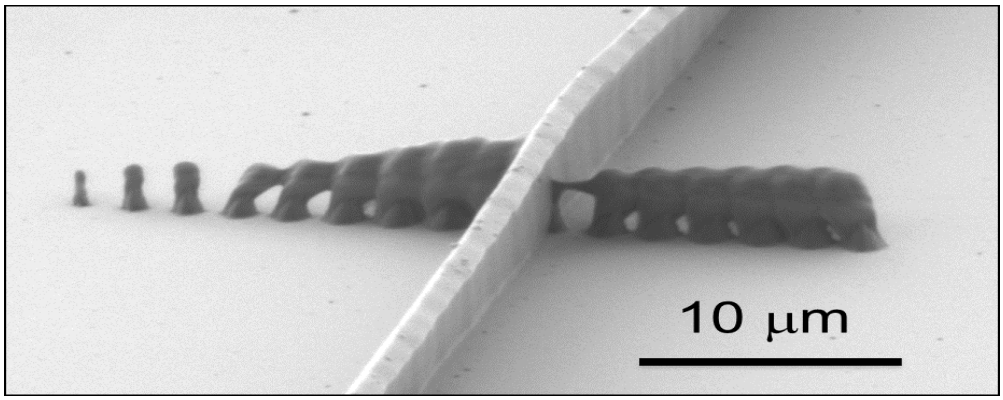

Figure 1.3 SEM image of SR399 showcasing the Memory effect[3]

Heat and laser scattering may also contribute to the memory effect. The range of the memory effect is 10's of microns, and the impact it has on mutating size can be reduced by prolonged pauses separating laser exposures referred to as hiatus time (Figures 1.4). However, hiatus time lengthens the fabrication process.

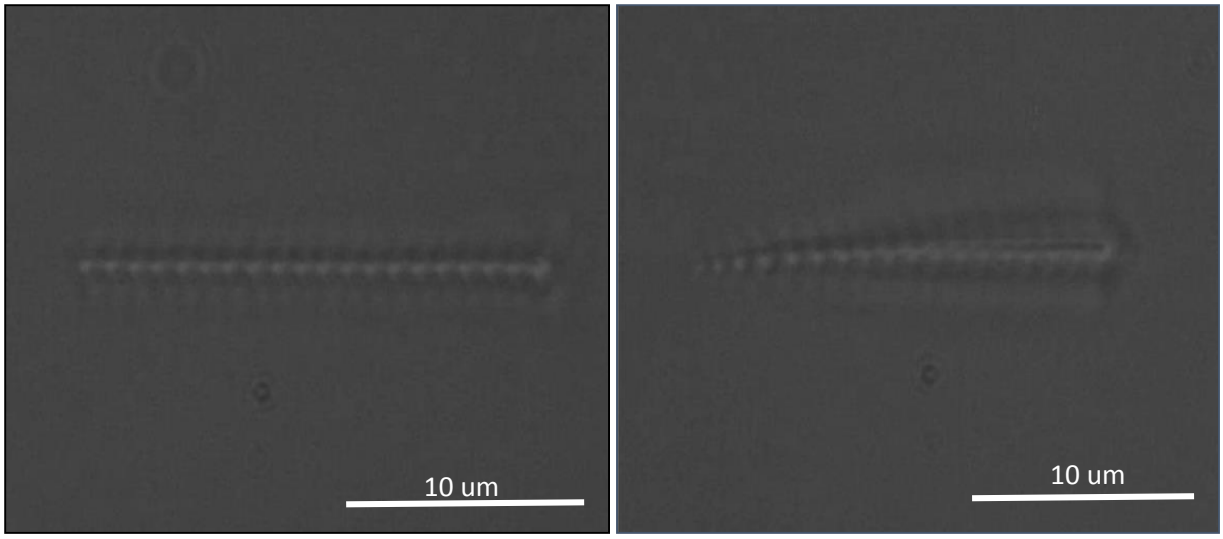

Figures 1.4 Both DLW camera images show a row of SR499 dots polymerized 1 um apart and each dot was exposed for 1 s each. The row of dots on the left had a hiatus time of 10 s. No memory effect can be observed. The row of dots on the left had the fastest hiatus time possible, 25 ms, and a profound memory effect can be observed.

Lithographing anything longer or larger than a feature with a length or diameter of a few micrometers cannot benefit from hiatus time. For example, a line with a length of 10 micrometers lithographed in one sitting widens as the laser beam progresses across the slide's surface.

The results of tuning DLW variables is difficult to analyze. The quality of a microstructure exterior can only be estimated from an image from an SEM or the DLW camera during fabrication. Not only is the degree of surface polymerization assumed, but also the interior, sides, and base of the structures are unexplored. Regular polymerized features and features that are a consequence of the memory effect are indistinguishable to the eye. Analyzing structures after fabrication is daunting when poorly polymerized features are washed away by solvents for development and the electron beam of the SEM can be powerful enough to leave impressions on the structure. My summer research aimed to shed light on the polymerization process, especially the memory effect. If scattering free radicals are the culprit of the memory effect, then barriers dividing polymerized features that block free radicals should cancel the memory effect. I designed a microstructure made from SU-8 2025 during BSRI with Bard's DLW setup to serve as a wall when polymerizing SR499.

Unfortunately, the SU-8 walls were not sealed so unintended polymerization of SR499 occurred over the walls seeping in between the barriers (Figures 1.5).

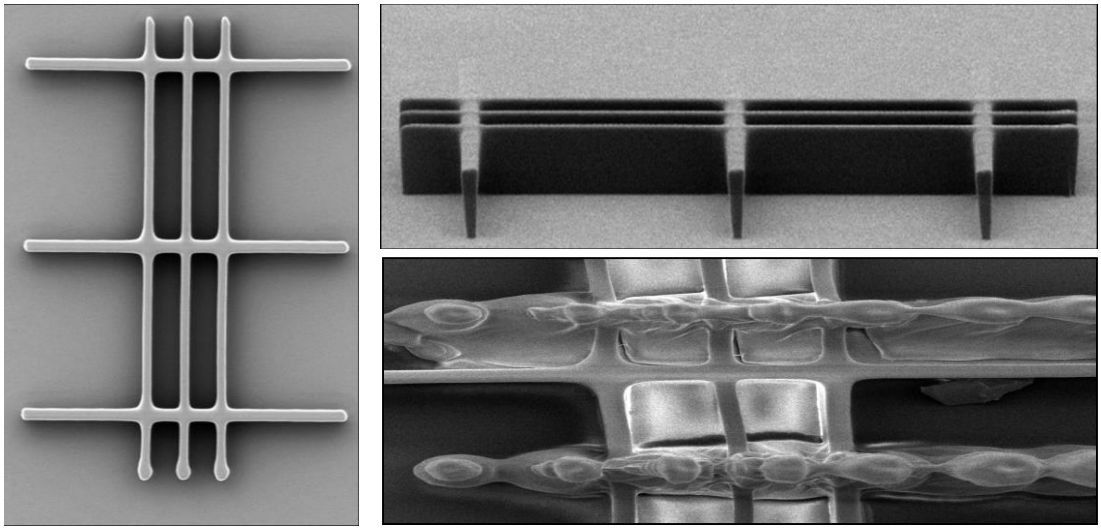

Figure 1.5 The SEM images are of microstructures from the top down and the side made of NOA 81 microtransfer molded from a PDMS stamp of the original SU-8 2025 prototype. The structures are 25 um tall, the horizontal walls are 130 um wide, and the vertical walls are 200 um long. The bottom right image shows SR499 dots polymerized in between and over the walls.

Raman Spectroscopy

The nature of the memory effect mechanism remained a mystery, but I gained a lot of experience with lasers, microscopy, and various acrylate resins. I had read before that spatially offset Raman spectroscopy (SORS), a derivative of Raman spectroscopy, was a recent technique developed for the analysis of paintings, which garnered my interest. Professor LaFratta was unable to imagine research that included art restoration work, but realized that Raman was the only form of spectroscopy that could properly analyze DLW microstructures. The DLW setup in the basement of the RKC had been previously converted into a Raman spectrometer for Min Kyung Shinn's Senior Project called *Fabrication and Characterization of Graphene-Boron Nitride van der Waals Heterostructure* because Raman and DLW have similar setups.[4] However, the data collected with the spectrometer had too much noise interference and aligning the instruments was

temperamental. The Raman spectrometer was only a small part of Min's project, so perfecting the system for versatile data collection was not a major concern. If a fully functional Raman spectrometer could be installed alongside the DLW, then microstructures could be analyzed during the fabrication process. Moving towards confident DLW fabrication requires designing a Raman spectrometer with a high signal to noise ratio, accessible operation, and consistent results.

Raman Mechanism[5]

In 1928, an Indian physicist named C.V. Raman discovered that a small fraction of photons scattering off an object were of a different wavelength than the incident light. This revelation was groundbreaking, providing further validation for the quantum theory of light behaving as both a particle and a wave. Few materials block out light completely, instead they absorb light to a certain depth. A molecule absorbs the photon exciting an electron from a ground state of energy to a *j* virtual state of energy (Figure 1.6).

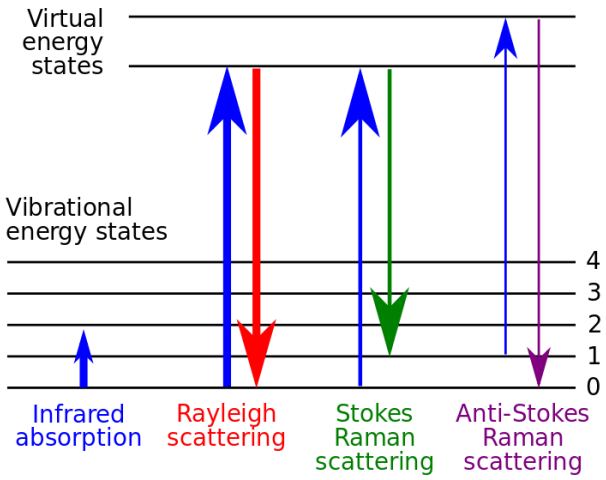

Figure 1.6 Raman scattering mechanism[6]

After ~10^{-15} s, a time corresponding to the period of one oscillation of the incident electromagnetic wave, a scattered photon is released from the electron returning to a ground state. 99.999% of excited electrons relax to the same ground state it started from releasing a photon of the same

wavelength as the incident photon, referred to as elastic Rayleigh scattering. The remaining 0.001% of excited electrons relax to a ground state of usually higher energy called Stokes scattering, and rarely relax to a ground state of lower energy called Anti-Stokes scattering. Rayleigh and Stokes scattering mechanisms are dependent on the same vibrational modes, but the processes that produce them are mechanistically different. Both Stokes and Anti-Stokes are responsible for the Raman signals, but Anti-Stokes is negligible since electrons infrequently populate anything other than the lowest ground state. Scattering causes a momentary distortion of electrons in a bond. Every molecule has its own individual spectrum of Stokes scattering determined by the unique symmetrical bond vibrational modes that result in a change of polarizability. Raman signals are similar to IR, except that IR signals are caused by a net change in dipole moment. Molecules with a center of symmetry have mutually exclusive IR or Raman active modes. Raman spectroscopy excels at analyzing inorganic materials for this reason. Overtone and combination bands are unusual in Raman, making them easier to read.

The equation for the energy of Stokes scattering is

$$E = h\,(\nu_{ex} - \nu_v)$$

Eq. 1 Energy of Stokes scattering photon

where ν_{ex} is the incident photon frequency and ν_v is the scattering photon frequency. Raman data is presented in a graph with the wavelength expressed as wavenumbers in reciprocal centimeters (cm^{-1}) versus intensity of the signal. Wavenumbers can be easily calculated with the equation

$$\Delta\omega = ((1/\lambda_o) - (1/\lambda_1))*10\text{^}7$$

Eq. 2 Raman shift in reciprocal cm from wavelength in nm

where λ_o is the wavelength of the excitation source and λ_1 is the wavelength of the scattering signal. Raman spectrometers will produce a graph with wavenumbers automatically, but the makeshift spectrometers I used read the signals in terms of wavelength and must be converted to

wavenumbers. Raman shift magnitude is not compromised by the color of the excitation source, as long as the source is not ultraviolet, which could cause the analyte to react or decompose, or of a wavelength that would cause the analyte to fluoresce, which would create signal interference. Furthermore, Raman emission frequency will equal the frequency of the excitation source raised to the fourth power if the analyte does not absorb any of the light.

The quality of DLW microstructures can be easily observed with Raman because the intensity of Raman signals are directly proportional to the concentration of functional groups. A larger concentration of an analyte's functional group receives a greater intensity of signal. Intensity is also dependent on the intensity of the source and the change in polarizability of bond vibrations among other things. Polymerization reactions link functional groups in monomers together, reducing the concentration of the monomers functional groups and increasing the concentration of the newly connected polymer functional groups. Common photopolymers, including SR499, have three peaks in a range of interest from 1550 cm^{-1} to 1780 cm^{-1} (Figure 1.7). The first signal is situated around 1593 cm^{-1} attributed to the aromatic ring vibrations of common photointiators. The second signal, and the most important of the three, is a sharp peak found around 1640 cm^{-1} indicating the C=C acrylate stretching mode that is cross-linked following activation by the photoinitiator. The intensity of the C=C stretching mode signal is a direct representation of the degree of polymerization. The final peak representing the carbonyl C=O stretching mode resides around 1714 cm^{-1}, which is a reference peak. Comparing the intensities of these peaks to reference spectra of unpolymerized photopolymer and a completely polymerized block of photopolymer, especially to the intensity C=C acrylate peak, we can analyze the quality of a microstructure features at micron-sized laser points. If the homemade Raman spectrometer can resolve these peaks that are disparaging by only 4 nm, then our goal will be met.

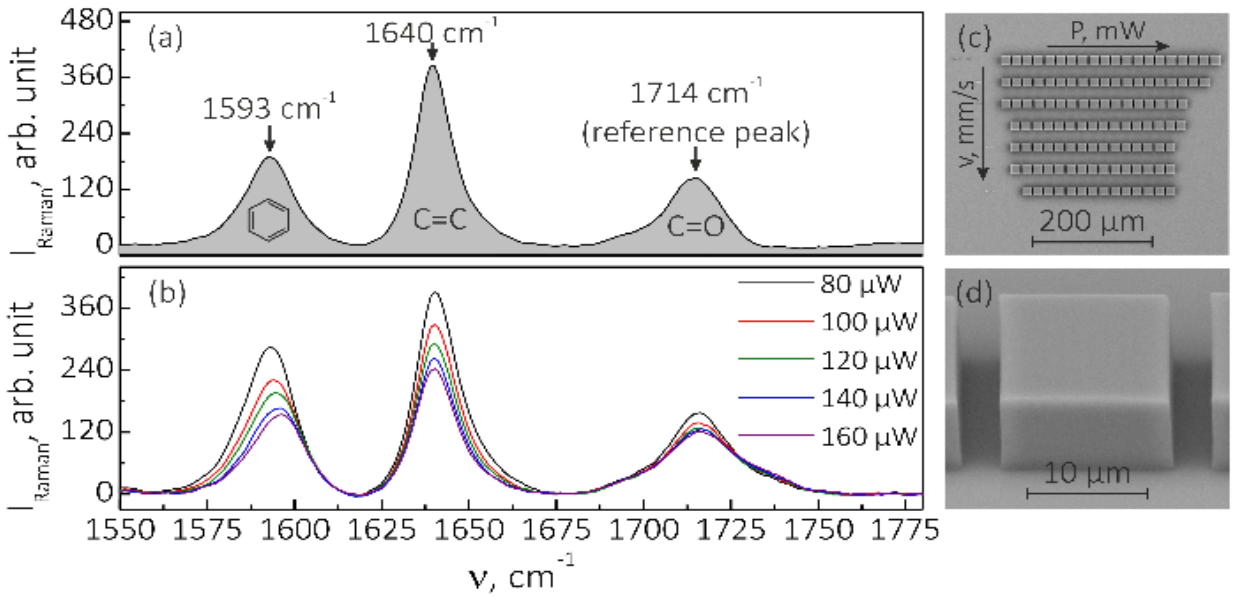

Figure 1.7 (a) Raman spectra of the pre-polymer and (b) evolution of the cuboids fabricated at 2.5 mm/s velocity. (c) SEM image of an array of the cuboids fabricated by means of TPP and (d) magnified image of one of them under 45 viewing angle.[7]

SORS[8]

The next step would be to employ a micro-SORS technique with our homemade set-up. Micro-SORS was originally designed for investigating layers of paint in fine art, but it was not until March of 2015 that Conti et al. successfully applied micro-SORS to noninvasively and nondestructively research thin turbidly scattering layers of materials such as wheat seeds, paper, and polymers. Basic Raman spectroscopy methods can only collect data of the surface of an object, while SORS can analyze any point within an object. Bomb squads use SORS to safely detect explosives within sealed containers. The concept of SORS is rather simple and ingenious. A spectrum of the surface of an object, referred to as a conventional "imaged" position, is taken directly above the point of interest within the object. Depending on the depth of the point of interest, a number of "defocused" spectra are taken from the surface to the point of interest, where the laser point and Raman collection areas are broadened. This is achieved by distancing the microscope objective by "defocusing distance Δz," hence the title spatial offset. A scaled subtraction of the

"imaged" spectrum from the "defocused" spectra results in a Raman spectrum of the point of interest without interference from the layers above (Figure 1.8).

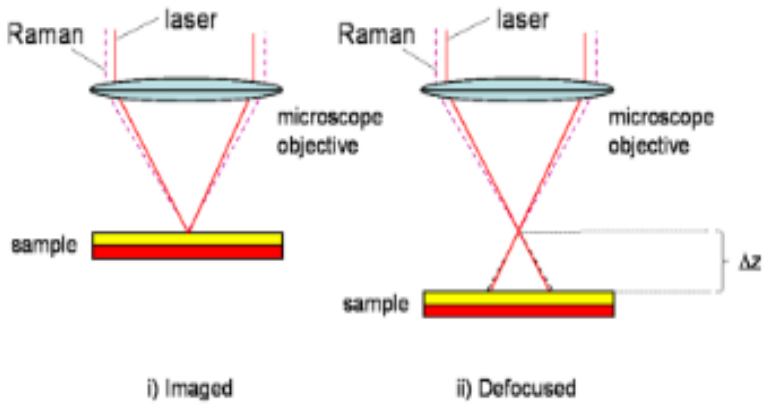

Figure 1.8 SORS technique[8]

Stronger laser powers and faster acquisition times can be used to make up for the reduced signal in the "defocused" spectra because the laser excitation area is more spread out. Parts of microstructures that are directly attached to the substrate can only be accessed with micro-SORS. If there are issues with a microstructure's adhesion to the substrate, we would never know until the microstructure falls off without micro-SORS. Sides of a microstructure are also areas of concern, which are hard to see with most spectroscopy methods. Fabricated walls could taper off close to the substrate surface for example, which would never be revealed without micro-SORS. Entire maps of every micron thick layer of an object can be made after thousands of spectra are taken across a sample, which is called hyperspectral imaging. Perhaps in the future, micro-SORS can be used to precisely image clusters of RNA and DNA helixes.

1.4 Raman microscopy[9,10]

A Raman microscope has five necessary components: an excitation source, a microscope, a chromatic filter, a spectrometer, and a computer. The laser is focused through the microscope irradiating a mounted sample. Scattering photons are passed through a filter and a spectrometer

that rejects Rayleigh scattering. A detector, such as a photomultiplier tube (PMT) or a charge coupling device (CCD), receives the scattering photons and a computer translates the data into a spectrum (Figure 1.9).

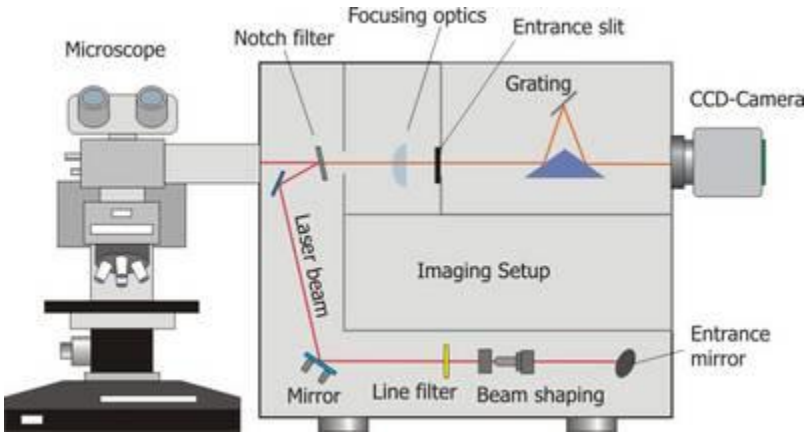

Figure 1.9 Simple Raman microscope[11]

The popular excitation laser sources are argon ion emitting 488 or 514.5 nm, krypton ion emitting 530.9 and 647.1 nm, helium-neon gas emitting 632.8 nm, an electrically pumped diode emitting 785 or 830 nm, and Nd:YAG (neodymium-doped yttrium aluminium garnet; $Nd:Y_3Al_5O_{12}$) crystals emitting at 1064 nm. Short wavelength sources improve Raman signal intensity because they avoid sample absorption, but run the risk of photodecomposition in the sample. Long wavelength sources are near-IR and function with high laser power while not having enough energy to fluoresce the sample. Raman requires an extremely stable excitation source. Green 532 nm lasers are the best choice for signal sensitivity in inorganic molecules because fluorescence is no cause for concern. Organic molecules suffer from fluorescence and which can drown out the Raman signal.

Basic spectrometers take in light, divide it into a spectrum, and convert the signal as a function of wavelength (Figure 1.10).

Figure 1.10 Spectrometer schematic[10]

The entrance slit that accepts the light is key for resolution. Determining the correct slit width is given by the equation

$$W_i = (M^2 \times W_s^2 + W_o^2)^{1/2}$$

Eq. 3 Image width of entrance slit equation

where W_i entrance slit image width, M is the magnification of the optical bench, W_s is the entrance slit width, and W_o is the degree of the optical bench image broadening. An optical bench is a term for the cooperation of the slit, the grating, and the detector. The image width is crucial if it is larger than the CCD pixel width. Entrance slit height also effects resolution. When the resolution is satisfactory, the slit should be widened as much as possible to increase the amount of scattering photons collected. The light is collimated by a concave mirror, then splayed out across various angles by a grating. Ruled gratings, a reflective material covering many parallel grooves, are inexpensive but have many imperfections that result in errors. Holographic gratings are formed on concave optical glass by crossing two UV beams that etch a sinusoidal pattern. The spectral response is more cohesive, but less efficient. The periodicity and amount of grooves in a grating plays a part in resolution and wavelength range. A second concave mirror directs and focuses the light into the CCD. CCDs in spectrometers require long integration times to collect a substantial

amount of scattering photons. Micron thick CCDs reduce the chance of the same electron being reabsorbed more than once, which muddles the outcome of the signal. Thermoelectric cooling, which utilizes the Peltier effect of electron flow heat transference between two conductors, can increase the integration times of the CCD, giving the spectrometer a more dynamic range and nearly eliminating dark noise count.

The objective lens and the chromatic filter have less reason for variation. The greatest magnification of an objective lens is preferred, since a laser beam is more tightly focused as the magnification increases. Chromatic filters need to block out light from a few nanometers above the excitation source wavelength and every wavelength below to ensure Rayleigh scattering and the excitation source does not interfere with the weak Raman signal.

The different configurations of Raman are countless and can be adjusted to meet the needs of any analyte by changing the excitation source, components of the spectrometer, microscope resolution, and computer program. The amount of Raman techniques are just as numerous as the combinations of Raman components. Portable Raman spectrometers are common market items. Some of these techniques will be discussed later on besides SORS. Our Raman spectrometers follow a basic configuration. A 633 nm laser is directed and enlarged through a series of tabletop mirrors and lenses into a microscope with a monochromator aligned where the microscope camera used to be. Our monochromator grating is controlled with an attached Arduino board. The Raman spectrum computer program was programmed in LabView from scratch. What makes our Raman microscope unique is a chopper and a lock-in mechanism to isolate the Raman signal and reduce noise. Furthermore, commercial Raman spectrometers are self-contained, while ours places the components together by hand. A commercial fluorimeter was converted into a basic Raman

spectrometers to collect reference spectra for comparisons between setups. Both set-ups will be explained in more detail in the experimental section.

1.5 Raman Resolution[12]

The possible spatial resolution of a Raman microscope relies on laser wavelength and microscope objective, given by the equation

$$\text{Spatial resolution} = 0.61\,\lambda \;/\; \text{NA}$$

Eq. 4 Raman spatial resolution

where NA is the numerical aperture of the microscope objective and λ is the wavelength of the excitation source. Unfortunately, Raman microscope spatial resolutions are afflicted by more variables than laser wavelength and microscope aperture. The interface of an analyte could cause the excitation source to produce scattering that strays far out of alignment. As the spectrometer focal length increases, the distance separating grating and detector, so does the spatial resolution. A higher number of grooves per millimeter in a diffraction grating makes for a higher spectral resolution. Smaller pixels in a detector achieves a higher spectral resolution. Since we will be observing polymer features as small as 1 um, the spatial resolution must be smaller than 1 um. Typical Raman microscope resolutions are 1 um, but our Raman microscope is atypical. Our Raman microscope needs a spatial resolution of less than 1 um and must be able to make a distinction between peaks that are less than 4 nm apart. With the limited resources available at Bard, getting a homemade Raman microscope to produce graphs of this quality is a major endeavor.

Experimental

Fluorimeter converted into a Raman spectrometer

A Quantamaster 300 Phosphorescence / Fluorescence Spectrofluorometer was converted into a Raman spectrometer to collect reference spectra to compare to spectra taken with our Raman microscope setup. The high powered lamp was excluded from the experiment because it is not monochromatic. A 532 nm diode laser with a heat controller and power controller was positioned next to the monochromator. An adjustable mirror was placed in front of an uncapped circular hole in the sample container box to be able to expose the sample cuvette at the correct angle. The opening leading to the monochromator was covered with a 535 nm long pass filter (Figure 2.1).

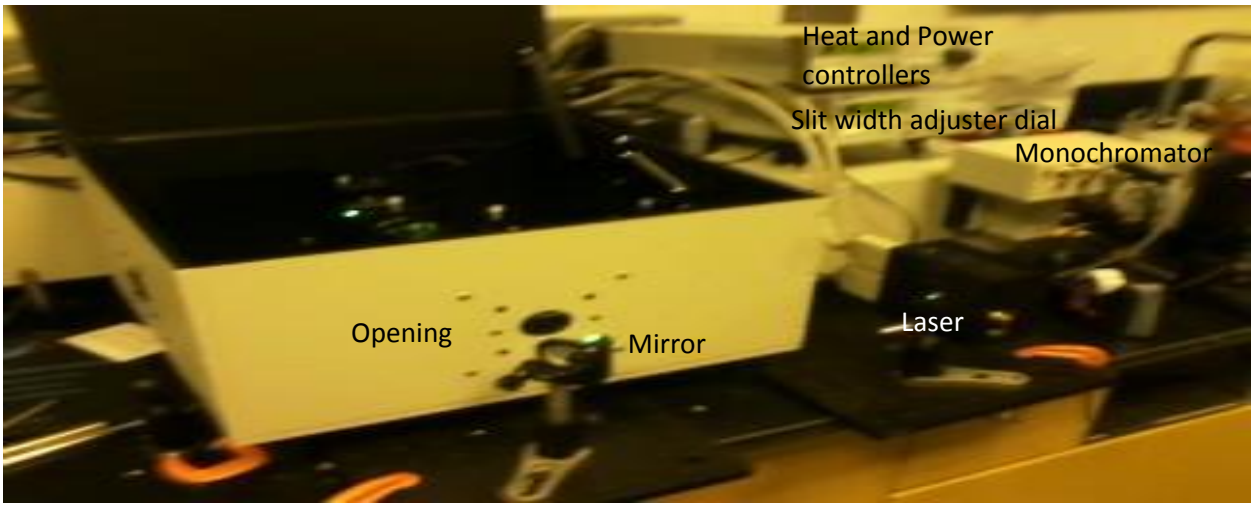

Figure 2.1 Fluorimeter/Raman set-up

Cyclohexane is a simple molecule with an immediately identifiable group of peaks, so this molecule was used to optimize the parameters of the converted fluorimeter (Figure 2.2).

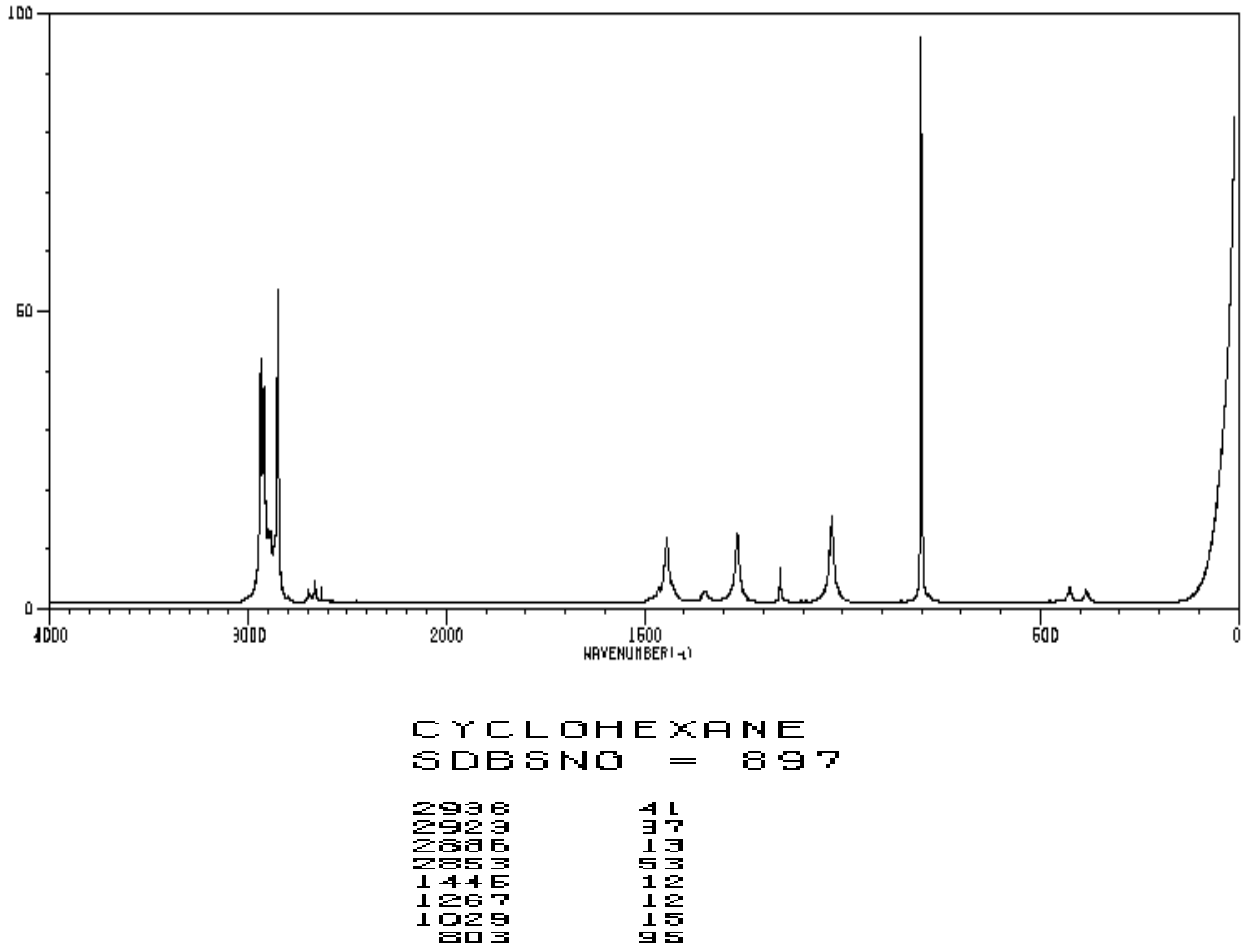

Figure 2.2 Cyclohexane reference Raman spectrum[13]

Cyclohexane served the same purpose for our Raman microscope. The width of the slits on either end of the passage separating the monochromator from the sample container were adjusted equally to optimize signal clarity. Reference spectra of unpolymerized and polymerized acrylate SR499 with 1% w/w addition of TPO-L photoinitiator were collected. The unpolymerized mixture was held in 4 ml UV vis cuvette with clear sides, as well as the cyclohexane. Polymerized SR499 was prepared in a glass vial under a UV lamp for a few minutes until it was solid. A large piece of polymerized SR499 was placed into the cuvette holder. Acquisition times were also varied on the spectrometer computer program to observe their effect on signal to noise ratio.

Procedure to convert DLW into Raman microscope

The entire DLW set up is spread out on an optical table for thermal stability and vibrational damping. A series of mirrors occupy half of the table to direct the UV beam into the microscope. Laser alignment must be maintained by keeping the beam centered on each mirror. The alignment cannot be disrupted, especially when the UV beam and Raman excitation source must be switched with ease for analysis to be carried out in between fabrication. A polarized 632.8 nm Thorlabs laser Model No. HNL210L with a 21 mW operating power and a 120 VAC power supply was used as the excitation source. Two beam expander lenses are mounted as far apart as possible to gain the largest beam size possible, ensuring maximum exposure through the microscope. Other mirrors are kept out of the path of the UV beam and were aligned with a ruler. The last mirror before the microscope opening had to block the UV beam path, so the mirror was placed on a hinge that switches the laser set up back to DLW when flipped down (Figures 2.3).

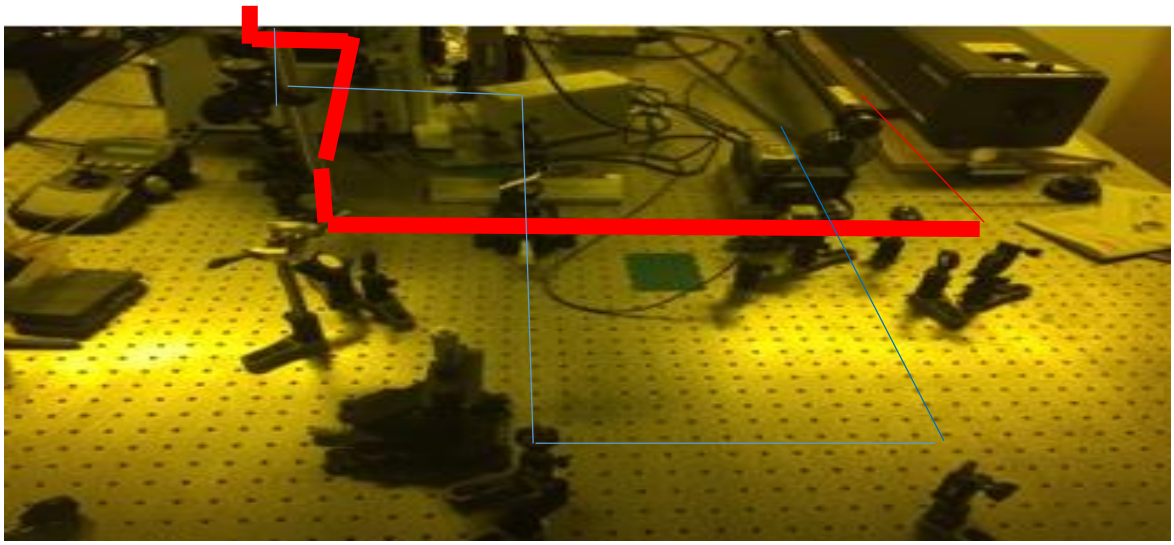

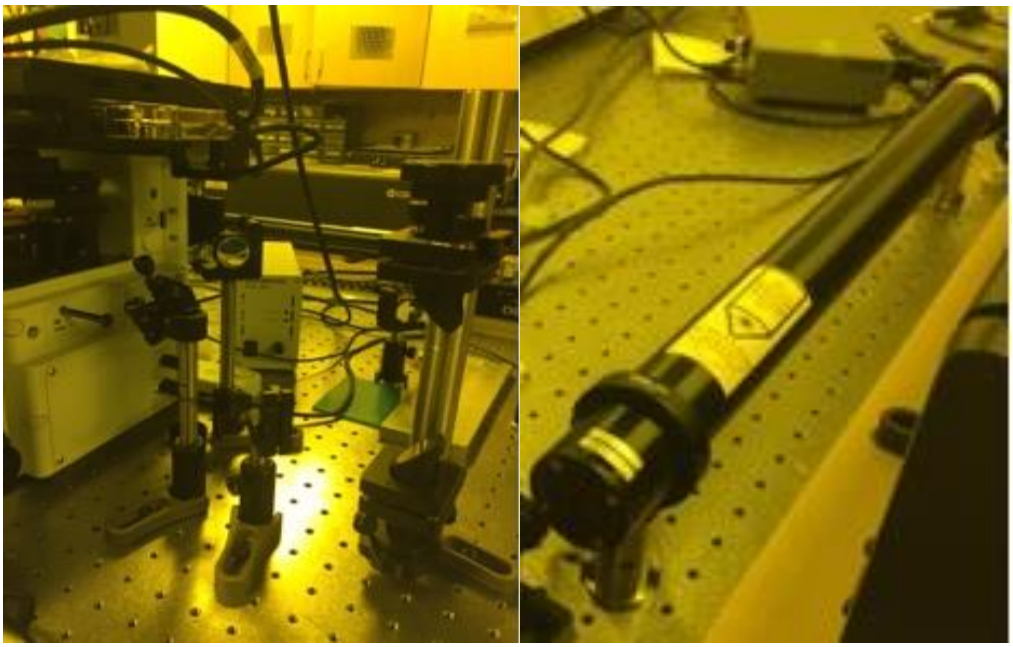

Figures 2.3 Paths of red and UV laser, flip mirror, and 632.8 nm laser

The confocal microscope is an Olympus IX71 model. Slides are mounted on the motorized stage and cuvettes can be laid sideways on the stage above the microscope objective. The objectives to choose from are 4×, 10×, 20×, 40× air, and 40× with oil. Since samples in cuvettes were primarily analyzed, the usual objective used was the 20×. A 640 nm long pass filter was used to block Rayleigh scattering and the excitation source from exiting the microscope (Figures 2.4).

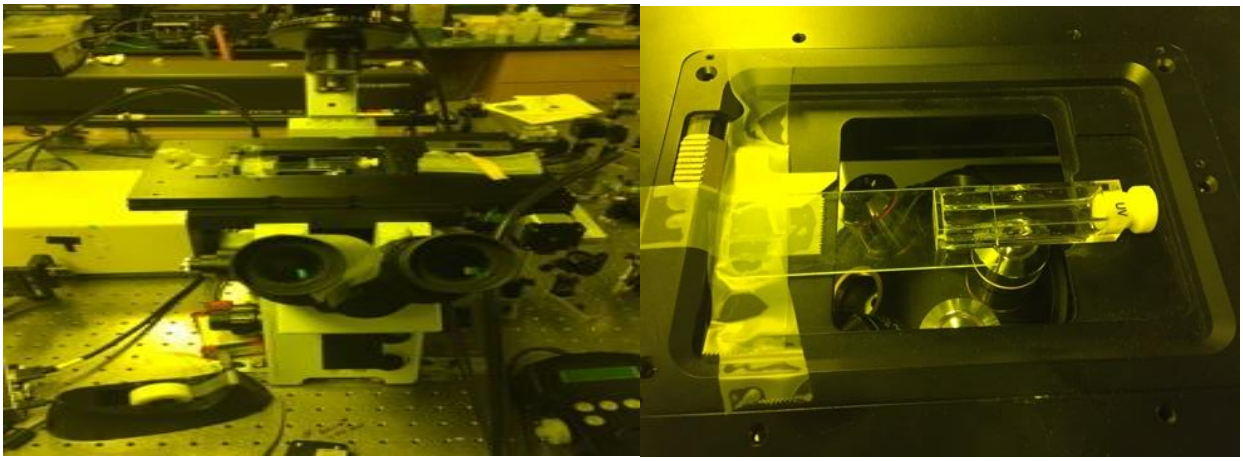

Figures 2.4 Microscope and stage

The microscope camera was removed and replaced with an adjustable concave mirror to prevent chromatic aberration and direct the scattering signal into the monochromator (Figure 2.5).

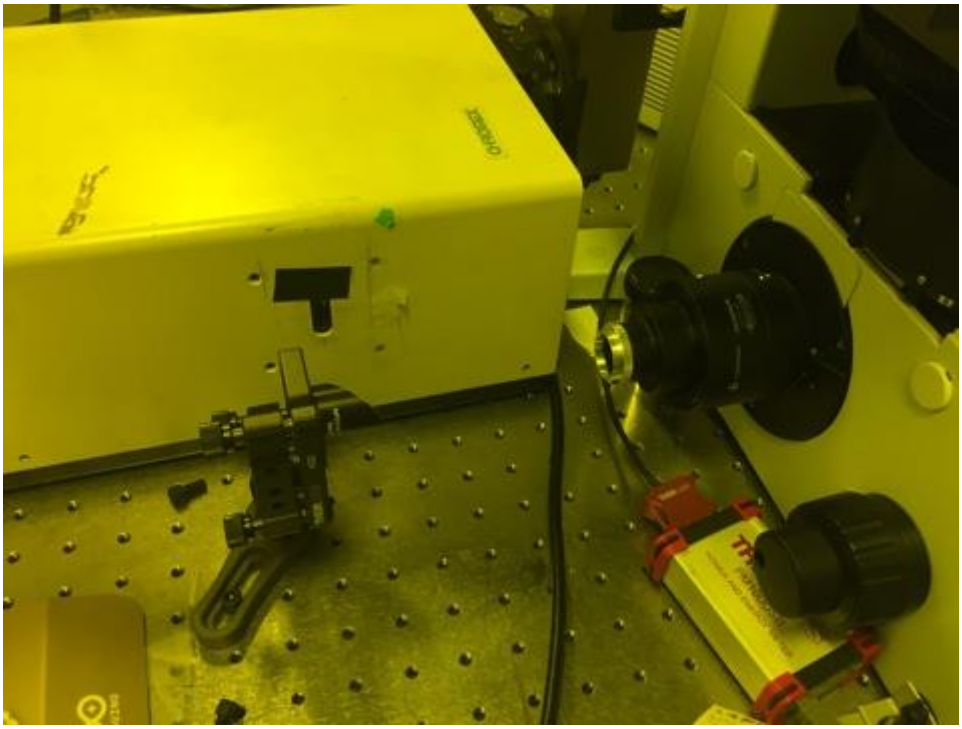

Figure 2.5 Monochromator, mirror, and microscope opening for scattering

The scattering light is very weak and nearly invisible to the naked eye, even with the room lights turned off. Highly fluorescent dye Atto 633, which fluoresces and scatters a visible red beam of light when excited with a wavelength of 633 nm, was used to align the monochromator entrance slit with the scattering light. The monochromator is aligned by hand and then the mirror is adjusted until the photometer reads the strongest signal. Atto 633 was diluted in deionized water many times until the liquid was a very light green and was no longer overloading the PMT. The Atto mixture was placed in a cuvette and laid on the side of the stage. A glass slide was taped on one side of the motorized stage opening to prevent the cuvette from falling through and hold it up.

The monochromator is an older Chromex model and the years have not been kind to it. The stage that rotates the internal grating and determines what wavelength of scattering light being collected broke long ago (Figure 2.5).

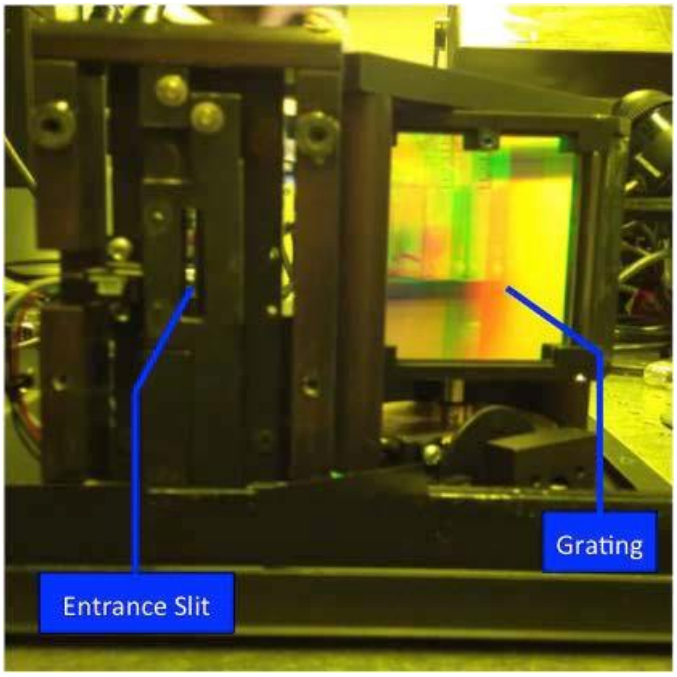

Figure 2.5 Chromex interior[4]

Professor LaFratta installed an Arduino board and programmed a LabView application to produce spectra (Figures 2.6).

Figures 2.6 Arduino board and LabView program

Although the missing components were effectively replaced, the monochromator sometimes malfunctions. The smallest entrance slit width available of 0.25 mm was chosen. A Pacific Instruments Model 126 photometer reads the signal as a function of voltage and inputs it into the LabView application. The monochromator cannot make a distinction between any wavelength of light, so the monochromator must be calibrated with a green 532 nm laser pointer. A folded kimwipe is taped over the entrance slit to avoid overexposure from the pointer which would photobleach and overload the PMT. When a prominent peak is seen in LabView, the monochromator can be calibrated to the wavelength of 532 nm. The stage can be rotated at increments of 0.3 nm to make sure the monochromator is never decalibrated by more than 0.3 nm. To further calibrate the instrument, a red 650 nm laser pointer is directed through the entrance slit. If a peak is produced when LabView says the monochromator is projecting signals at around 650 nm, then experimentation can proceed. Before any procedure begins, the monochromator must be calibrated. Data collection on cyclohexane and SR499 was attempted, but did not yield trustworthy data.

Signal optimization changes (lock-in/chopper)

The monochromator was subject to noise interference of a magnitude of ~0.2 V when the room lights were left on, so initial work was carried out in the dark. However, light from the LEDs of the surrounding instruments and the computer monitor also interfered with data collection. The method we chose to reduce noise was with a chopper, a model SR540 chopper controller and a Stanford Research Systems Model SR830 DSP lock-in amplifier. A lock-in amplifier uses phase-sensitive detection that will only read signals as small as a few nanovolts at a frequency of the chopper. The chopper is a circular piece of metal with small periodic openings around the outside which rotates at high frequencies. The 633 nm laser is passed through the

openings and is chopped up at the same frequency of the spinning chopper. The chopper is placed directly in front of the laser. The lock-in amplifier will only receive scattering signals at the chopper frequency and amplifies the signal. The sensitivity of the lock-in amplifier can be adjusted from as high as 500 volts to as low as 1 nanovolt. The time constants, or the increments of time between every signal read, can be adjusted from as fast as 10 us to as slow as 300 ks. The right combination of these two parameters is key to our spectrometer eliminating noise and resolving the necessary peaks. If the sensitivity is too high and the time constant is too slow, the signal input can overload the lock-in mechanism. An input overload is anything above 1.4 Vpk. Many spectra of cyclohexane in a cuvette were taken varying the sensitivity and time constant until every cyclohexane peak was clearly resolved (Figures 2.7).

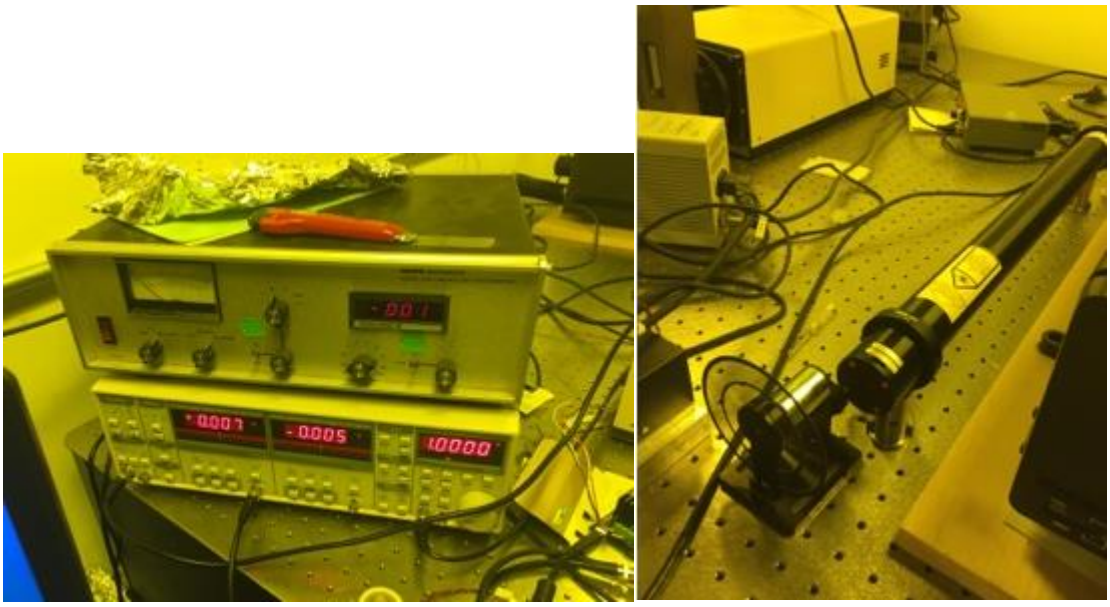

Figures 2.7 Photometer on top, Lock-in on bottom, chopper in front of the laser

Results

Raman spectrometer from fluorimeter: pros/cons/limitations

The fluorimeter had excellent signal to noise ratio since it was in a contained system that blocks out room light. Data collection was reliable and graphs were reproducible. Each graph took a matter of seconds to produce.

Laser alignment required a great deal of trial and error by irradiating cyclohexane and adjusting the mirror until the first peak at 2949 cm^{-1} reached an intensity of a little over 2.5E5. There was no way of telling where the laser should be angled to get the highest intensity until a spectrum would have such intense signals.

The limitation was that this set-up is a Raman spectrometer and not a Raman microscope. The spatial resolution of the beam is quite large without an objective lens to magnify the beam. Microstructures could never be analyzed in this set-up, only bulk materials in cuvettes or appropriately sized solid chunks that would fit in the cuvette holder.

Raman microscope from DLW: problems encountered

Research did not get very far because of the bugs in the monochromator. There were multiple instances of spectra going haywire or disappearing while trying to optimize the set-up by analyzing cyclohexane. Sometimes it was merely an issue of requiring recalibration, which can be a lengthy process disrupting work. Sometimes the Arduino boards would crash the

computer program because the circuits would touch the grounded metal table and short out. The computer would have to be restarted and the monochromator would have to be recalibrated just to be safe. Once, the grating was misaligned and caused the green laser pointer used for calibration gave off eight different peaks instead of a single peak as it should, making even calibration impossible. The last time I tried to collect cyclohexane spectra, the signal randomly flatlined and after two hours of troubleshooting, I decided to stop. The chopper was able to cancel enough noise to be able to work with room lights on. Regardless of whether or not the lights were left on, noise would spike on the lock-in from zero V to around +0.5 V when very powerful peaks would be read. These issues made all research inconclusive, since it was unclear how much the set-up had changed after each monochromator malfunction. Each spectrum was incomparable.

Ways to improve the set-up

It goes without saying, but having a new fully functional spectrometer would have improved the research. However, a lot of work would still have to be done to tweak the set-up until it was good enough to analyze microstructures. Plans were made to bring in an air purifier to remove floating dust particles that would disrupt the path of the laser. Lock-in amplifier setting combinations of voltage and time constant would have to be tested until the clearest signals could be achieved. Different slit sizes would also need to be varied to get the best results.

Other inexpensive and simple Raman techniques would improve spectra. Inverse-SORS has a donut shaped beam to excite sources. A regular laser beam creates scattering spread out in a circle at every angle. A monochromator entrance slit can only be placed in a single position to collect scattering around the beam excitation site, so a large percentage of Raman scattering is never collected. The donut shaped beam works in reverse, exciting a circular area that causes

scattering to be concentrated in a single beam directly upward. Surface enhanced Raman spectroscopy (SERS) uses colloidal gold or silver solution mixed in with the analyte, or a substrate coated in layer of gold or silver that is a few nanometers thick, to increase the intensity of Raman signals by as much as 10^{14}. The mechanism is still contested, but it has to do with plasmon resonance, which is a wave of oscillating electrons that propagates in a direction parallel to the dielectric material interface (Figures 3.1).

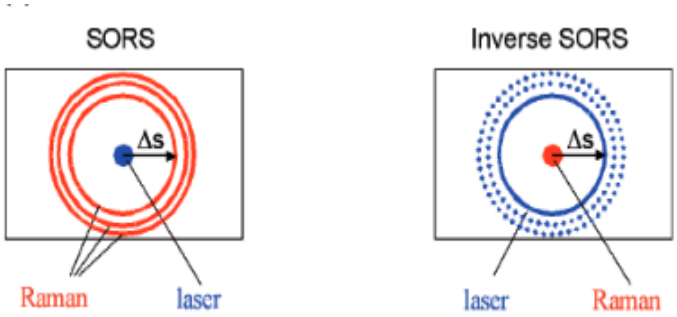

Figures 3.1 SORS and Inverse SORS schematic

Data

Fluorimeter

After taking many spectra of cyclohexane it was discovered that the best slit size for the fluorimeter was 0.6 mm. Changing the acquisition time did not change signals. New set-up means with the 532 nm laser (Figure 4.1).

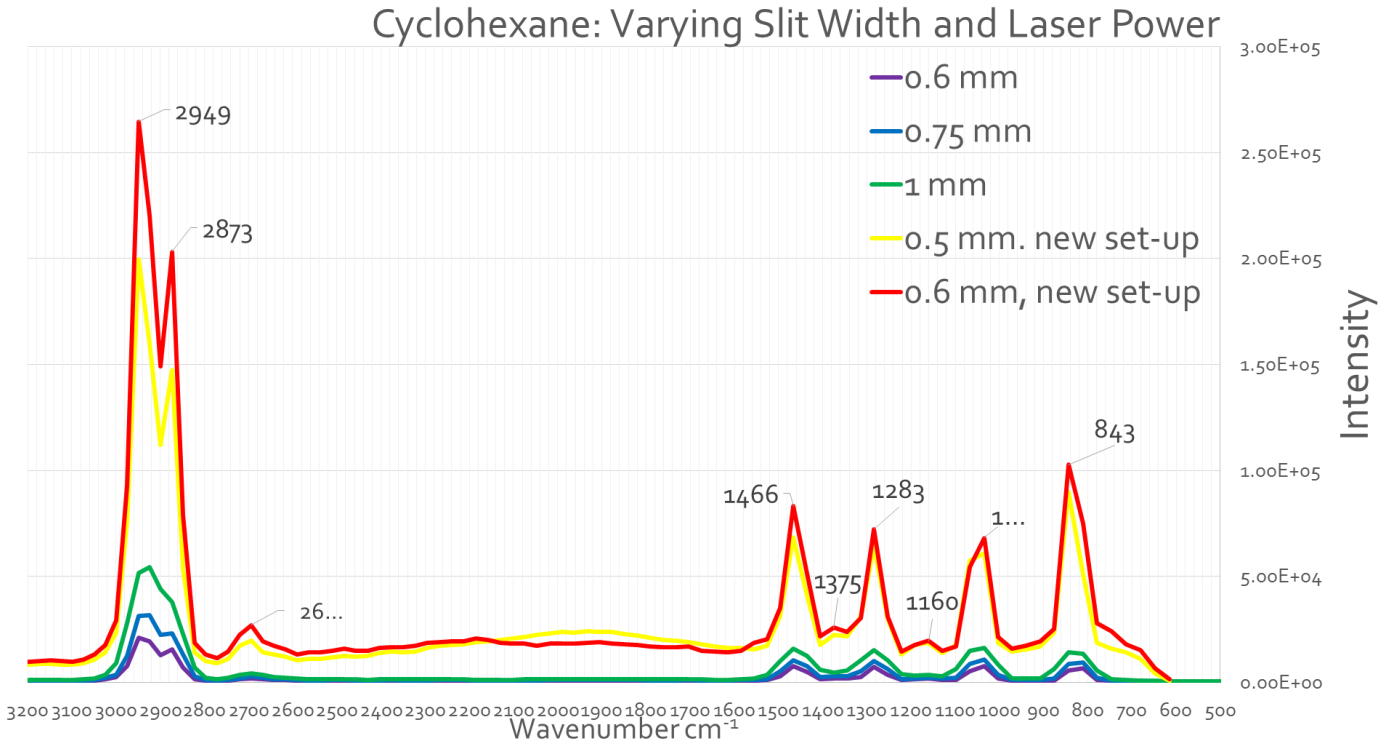

Figure 4.1 Varying slit width

A comparison of polymerized and unpolymerized SR499 shows the peaks clearly dissipating, including the important peaks at 1732 and 1644 cm^{-1}. The nature of the huge slope may be due to the mixture of photoinitiator, polymer, and inhibitor blending together.

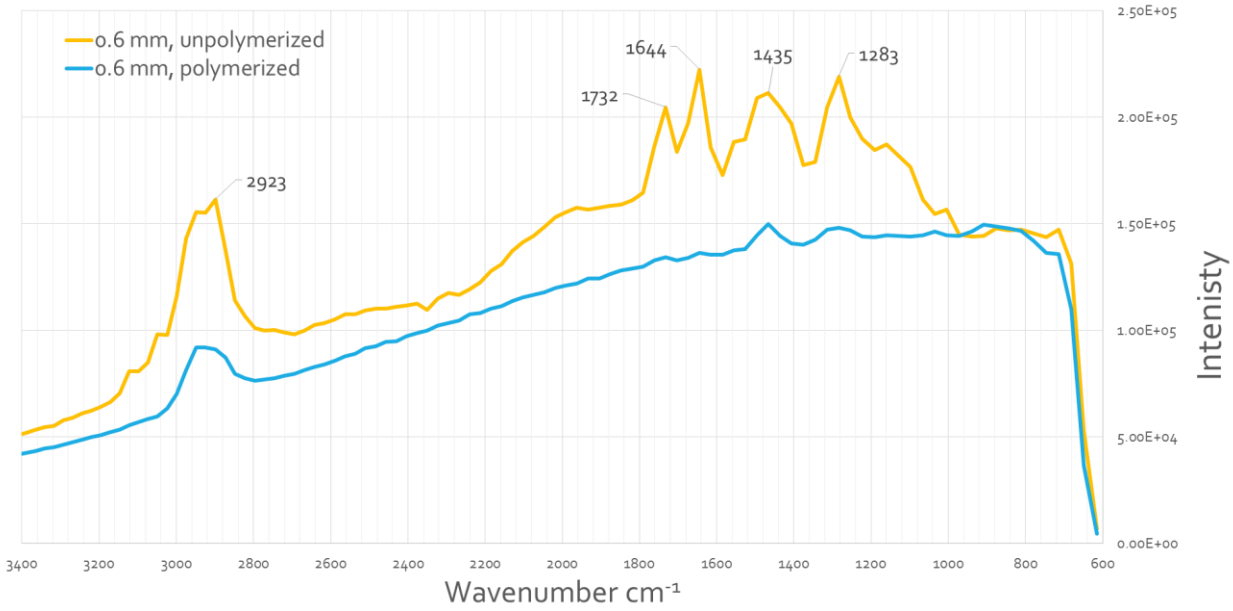

DLW Raman microscope

Not much to be said about this data because of the monochromator.

Conclusion

Although I am somewhat disappointed with how research went due to monochromator malfunctions, I learned a lot about how Raman spectrometers work and how they can be made from scratch. This is an incredibly useful skill to have in an art restoration career, not to mention in the world of analytical chemistry. At the Marist ACS conference in April where I presented the progress of my research, many peers and professors marveled at the challenge I had taken on of creating a functional Raman microscope from scratch. Professor LaFratta was always around to help and keep my confidence up. If I had the chance to work on making another makeshift Raman microscope, I wouldn't hesitate for a 10^{-15} of a second.

References

(1) Zhang, Y.-L.; Chen, Q.-D.; Xia, H.; Sun, H.-B. *Nano Today* **2010**, *5* (5), 435–448.
(2) "Photopolymer." Wikipedia. https://en.wikipedia.org/wiki/Photopolymer
(3) Photo courtesy of Professor LaFratta
(4) Min, K.S. "Fabrication and Characterization of Graphene-Boron Nitride van der Waals Heterostructure*". Bard Commons Senior Project Reserves.* **2014.**
(5) Skoog, D. A.; Holler, J. F.; Crouch, S. R.; HOLLER. *Principles of instrumental analysis*, 6th ed.; Thomson Brooks/Cole: United States, 2006.
(6) "Raman spectroscopy." Wikipedia. <http://en.wikipedia.org/wiki/Raman_spectroscopy>
(7) Žukauskas, A.; Matulaitienė, I.; Paipulas, D.; Niaura, G.; Malinauskas, M.; Gadonas, R. *Laser & Photonics Reviews* **2015**, *9* (6), 706–712.
(8) Conti, C.; Realini, M.; Colombo, C.; Sowoidnich, K.; Afseth, N. K.; Bertasa, M.; Botteon, A.; Matousek, P. *Analytical Chemistry* **2015**, 87 (11), 5810–5815.
(9) Skoog, D. A.; Holler, J. F.; Crouch, S. R.; HOLLER. *Principles of instrumental analysis*, 6th ed.; Thomson Brooks/Cole: United States, 2006.
(10) Tek, W. Raman spectroscopy, modular Spectrometers, and OEM/OED solutions http://bwtek.com/ (accessed May 4, 2016).
(11) Raman microscopy http://www.ws.chemie.tu-muenchen.de/groups/haisch/techniques0/raman-microscopy/ (accessed May 4, 2016).
(12) HORIBA (1996) Raman FAQs - what factors affect spectral resolution in a Raman spectrometer? Available at: http://www.horiba.com/scientific/products/raman-spectroscopy/raman-academy/raman-faqs/what-factors-affect-spectral-resolution-in-a-raman-spectrometer/ (Accessed: 4 May 2016).
(13) http://sdbs.db.aist.go.jp/sdbs/cgi-bin/direct_frame_disp.cgi?sdbsno=897
(14) Matousek, P. (2006) 'Inverse spatially offset Raman spectroscopy for deep Noninvasive probing of Turbid media', *Applied Spectroscopy*, 60(11), pp. 1341–1347. doi: 10.1366/000370206778999102.